Final state parton shower for electron-positron annihilation

Author
Giovanni Parri

Supervisors
Prof. Dr. Massimiliano Grazzini
Dr. Luca Buonocore
Dr. Luca Rottoli

A thesis presented for the degree of
Bachelor in Physics.

Department of Physics
University of Zürich
September 2021

Acknowledgement

I would like to thank Professor Massimiliano Grazzini for giving me the opportunity to address this stimulating topic.
Many thanks also to Luca Buonocore and Luca Rottoli for always being precise and clear in their explanations and for being available and present during my months of work.

Contents

1 Introduction

The aim of this bachelor thesis is to simulate a parton shower in an electron-positron collision. At leading-order (LO) in perturbation theory, the process proceeds via annihilation of the e^+e^- pair into a boson Z or by a virtual photon, which then decays into a quark-antiquark pair. The generated quarks are very energetic and can therefore be treated as free particles. However, as they carry a color and an electric charge, the emission of gluons and photons due to bremsstrahlung is observed. The emission of photons can be neglected because the parameter $\frac{\alpha_s}{2\pi}C_{F,A}^2$ weighting the gluons emission is larger than $\frac{\alpha_{em}}{2\pi}e^2$, which regulates the bremsstrahlung. The gluons, in their turn, will split into a $q\bar{q}$ pair or in two other gluons, and so on. All the emissions are collinear, and in the final state a larger presence of gluons rather than quarks is observed, since the gluon Casimir $C_A = 3$ is larger than the Casimir of the quarks $C_F = 4/3$.
After the hard scattering, all the process is described by the parton shower, splitting by splitting, the energy is dissipated until it reaches low values, where the non-perturbative QCD effects become predominant and perturbation theory is no longer valid.

The process is characterized by many splitting lines and vertices. Each line has a weight which is determined by the Sudakov form factor $\Delta(t)$; to reconstruct all the momenta of this tree graph, we simply need the initial hard parton momenta and three variables z, t and φ, that we assign to each vertex. The first variable z characterises the fraction of the total energy that is distributed between the emitted partons. The second variable t allows us to order the shower, it can be the angle θ^2 between the two emitted partons, or the invariant mass Q^2, or -as in our case- it may be the transverse momentum p_T^2. The last parameter is the azimuth angle φ, which appears only as a constraint in the four-momenta conservation and it is inconsequential.

My presentation is divided in two main parts: the first one, explained in section 3, where we approach the topic in a simplified way by considering only the first splitting of the quark. In the second part, section 4, we implement instead a complete parton shower which exactly reconstructs the kinematics of the splittings applying a dipole-approach, where a fourth particle called spectator is involved in order to conserve the four-momentum of the branching process.

Lastly, different observables in an e^+e^- collision are measured. In particular, given the previous evolution of the parton shower and the fact that partons are collinear, the event in the final state contains jets. Therefore, we will focus on the jet multiplicity, its dependence on the energy of the collider and on the parameter of the jet algorithm. Starting from the results of the jets clustering, the mass and the transverse momentum of the Z-boson will also be reconstructed.
Finally, a thrust algorithm to study the shape of the finale state partons will be implemented.

2 Theory behind parton shower simulation

2.1 Hard scattering cross section at LO

The simplest e^+e^- process that generates hadrons is

$$e^+e^- \to q\bar{q}.$$

In the following, we perform the calculation of the hard scattering cross section at leading order (LO) of this reaction, considering only the diagram which involves the virtual photon. The difference between a cross section for lepton production, for example $e^+e^- \to \mu^+\mu^-$, is that each quark carries a different electric charge $Q|e|$ and a color charge, therefore one have to count each quarks N_c times. The quarks appear in 6 possible flavours: u, c, t quarks with $Q = \frac{2}{3}$ and d, s, b quarks that have $Q = -\frac{1}{3}$.
The matrix element to lowest order for $e^+e^- \to q\bar{q}$ and the the unpolarized cross section of this process is computed using the Feynman rules on the following diagram.

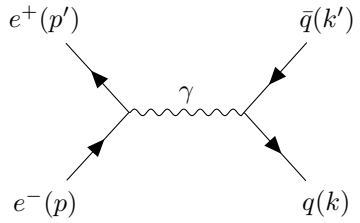

$$\begin{aligned} i\mathcal{M} &= \bar{v}^{s'}(p')(-ie\gamma^\lambda)u^s(p)\left(\frac{-ig_{\lambda\nu}}{(p+p')^2}\right)\bar{u}^r(k)(-iQe\gamma^\nu)v^{r'}(k') \\ &= \frac{iQe^2}{(p+p')^2}\left(\bar{v}^{s'}(p')\gamma^\lambda u^s(p)\right)\left(\bar{u}^r(k)\gamma_\lambda v^{r'}(k')\right) \end{aligned} \tag{1}$$

where s, s', r and r' are the spin indices.
This amplitude is only useful if we find its complex conjugate, which is proportional to the complex conjugate of a bi-spinor product $\bar{v}\gamma^\mu u$:

$$(\bar{v}\gamma^\mu u)^\dagger = u^\dagger(\gamma^\mu)^\dagger(\gamma^0)^\dagger v = u^\dagger(\gamma^\mu)^\dagger\gamma^0 v = u^\dagger\gamma^0\gamma^\mu v = \bar{u}\gamma^\mu v. \tag{2}$$

Thus, the squared matrix element is given by:

$$|\mathcal{M}|^2 = \frac{Q^2e^4}{(p+p')^4}\left(\bar{v}(p')\gamma^\lambda u(p)\bar{u}(p)\gamma^\mu v(p')\right)\left(\bar{u}(k)\gamma_\lambda v(k')\bar{v}(k')\gamma_\mu u(k)\right). \tag{3}$$

In most of the experiments the beams of electron and positron are unpolarized, for this reason the measured cross section is an average over the electron and positron spins s and s'. The detectors are also unaffected by polarization and it is difficult to control the spins of the final state. Therefore, the measured cross section is also a sum over the quarks spins r and r'.

$$\frac{1}{2}\sum_s\frac{1}{2}\sum_{s'}\sum_r\sum_{r'}|\mathcal{M}(s,s'\to r,r')|^2. \tag{4}$$

Next, we use completeness relations in order to simplify the amplitude squared formula:

$$\sum_s u^s(p)\bar{u}^s(p) = \not{p} + m \qquad\qquad \sum_s v^s(p)\bar{v}^s(p) = \not{p} - m, \tag{5}$$

where $\not{p} = \gamma_\mu p^\mu$.
The first bracket of equation 3 can be written as:

$$\begin{aligned} \sum_{s,s'}\bar{v}_a^{s'}(p')\gamma^\lambda_{ab}u_b^s(p)\bar{u}_c^s\gamma^\mu_{cd}v_d^{s'}(p') &= \sum_{s,s'}v_d^{s'}(p')\bar{v}_a^{s'}(p')\gamma^\lambda_{ab}u_b^s(p)\bar{u}_c^s\gamma^\mu_{cd} \\ &= (\not{p}' - m)_{da}\gamma^\lambda_{ab}(\not{p}+m)_{bc}\gamma^\mu_{cd} \\ &= \mathrm{Tr}\Big[(\not{p}'-m)\gamma^\lambda(\not{p}+m)\gamma^\mu\Big]. \end{aligned} \tag{6}$$

One can compute in a similar way also the second bracket; and neglecting the mass of the fermions we get:

$$\frac{1}{4}\sum_{\text{spins}}|\mathcal{M}|^2 = \frac{Q^2e^4}{4(p+p')^4}\text{Tr}\left[\not{p}'\gamma^\lambda\not{p}\gamma^\mu\right]\text{Tr}\left[\not{k}\gamma_\lambda\not{k}'\gamma_\mu\right]. \tag{7}$$

Using the traces theorems of the gamma matrices which states

$$\text{Tr}[\gamma^\mu\gamma^\nu\gamma^\rho\gamma^\sigma] = 4(g^{\mu\nu}g^{\sigma\rho} - g^{\mu\rho}g^{\nu\sigma} + g^{\mu\sigma}g^{\nu\rho}) \tag{8}$$

we get

$$\frac{1}{4}\sum_{\text{spins}}|\mathcal{M}|^2 = \frac{8Q^2e^4}{(p+p')^4}[(p\cdot k))(p'\cdot k') + (p\cdot k')(p'\cdot k)]. \tag{9}$$

Defining the Mandelstam variables

$$\begin{aligned} s &= (p+p')^2 = 2pp' = (k+k') = 2kk', \\ t &= (p-k)^2 = -2pk = (p'-k')^2 = -2p'k' \\ u &= (p-k')^2 = -2pk' = (p'-k)^2 = -2p'k \end{aligned}$$

one can write the squared amplitude in the following way:

$$\frac{1}{4}\sum_{\text{spins}}|\mathcal{M}|^2 = \frac{2Q^2e^4}{s^2}[t^2+u^2]. \tag{10}$$

In the center of mass frame, where the emitted quarks form an angle θ with the collision axis, the Mandelstam variables take on these values:

$$t = -\frac{s}{2}(1-\cos(\theta)) \qquad\qquad u = -\frac{s}{2}(1+\cos(\theta)).$$

Since this case is the one where two particles are generated after the scattering of two other particles, the differential cross section is (see Appendix A.2):

$$\begin{aligned} \frac{d\sigma}{d\Omega} &= \frac{1}{2E_\mathcal{A}2E_\mathcal{B}|v_\mathcal{A}-v_\mathcal{B}|}\frac{|\vec{k}|}{(2\pi)^2 4E_{cm}}\frac{1}{4}\sum_{\text{spins}}|\mathcal{M}|^2 \\ &= \frac{Q^2e^4}{32\pi^2 s}[1+\cos^2\theta], \end{aligned} \tag{11}$$

here $|v_\mathcal{A}-v_\mathcal{B}| = 2$, $E_\mathcal{A} = E_{cm}/2 = \sqrt{s}/2 = E_\mathcal{B}$ and $|\vec{k}| = \sqrt{s}/2$ was used.
Finally, taking $\alpha_{\text{em}} = e^2/(4\pi)$, we get:

$$\frac{d\sigma}{d\cos\theta} = \frac{\pi Q^2\alpha_{\text{em}}^2}{2s}N_c[1+\cos^2\theta]. \tag{12}$$

Up to now we have considered only the photon exchange diagram. In general, the Z-boson diagram has also to be considered. Therefore, to compute the matrix element of the process one have to evaluate the modulus square of a sum of amplitudes. The resulting differential cross section as generator of the $q\bar{q}$ pair can be written as:

$$\frac{d\sigma}{d\cos\theta} = \frac{\pi\alpha_{\text{em}}^2}{2s}[A_0(1+\cos^2\theta) + A_1\cos\theta], \tag{13}$$

where the coefficients A_0 and A_1 are defined in Appendix A.3.

The differential cross section of the hard process (13) acts as a probability distribution for the angle θ. In figure (1) the distribution of $\cos\theta$ depending on the flavor of the quarks is shown. The behaviour of the histograms is similar in both panels; however, the probability that a

quark d, s or b is produced is $\frac{1}{4}$; while, removing the t quark, the probability of generating a u or c quark is $\frac{1}{8}$.

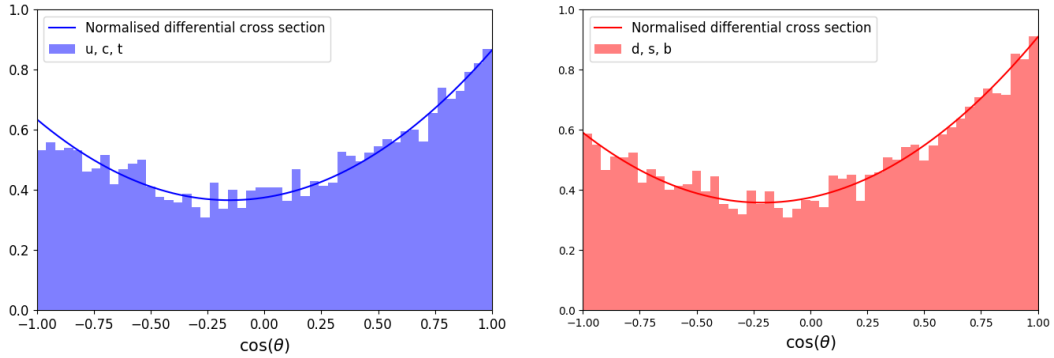

Figure 1: Normalised distribution of the direction of the quark after an e^+e^- collision at $E = M_Z$. Quarks u, c and t in the left panel, quarks d, s and b in the right panel.

With the polar angle θ and an arbitrary azimuthal angle $\varphi \in [0, 2\pi]$, the four momenta of the two emitted particles in the center of mass frame $(p + p')$ can be found. The azimuthal angle φ is chosen randomly since the reaction is symmetric with respect to the collision axis.
From these momenta we can start to develop our parton shower; where various gluons, quarks and antiquarks will be emitted.

2.2 Collinear limit and factorization

After the hard collision, we observe the emission back to back of a quark and its antiparticle and we expect a lot of final state particles produced by splittings of the type $a \to bc$. We refer to the collinear limit when the angle (or the transverse momentum) between the two emitted partons becomes small. The probability of this type of emission is high. Therefore, in this limit, one can factorize the cross section of the branching process into the product of a cross section times a splitting function. Considering a decay with $n+1$ final state particles where the final state gluon becomes collinear to a final state quark, we get that the cross section can also be written as:

$$|M_{n+1}|^2 d\Phi_{n+1} \Rightarrow |M_n|^2 d\Phi_n \frac{\alpha_s}{2\pi} \frac{dt}{t} P_{qq}(z) dz \frac{d\phi}{2\pi}, \tag{14}$$

where M_{n+1} and M_n are the amplitude for the $n+1$ and n body process, z is the fraction of energy distributed between the quark and the gluon, $P_{qq}(z)$ is a splitting function and describes the probability that a splitting with energy fraction z will occur, t is the ordering variable and $d\Phi_n$, which is the phase space for n particle, is defined as:

$$d\Phi_n = \prod_{i=1}^{n} \frac{d^3 p_i'}{(2\pi)^3} \frac{1}{2E_i} \delta^4 \left(\sum_{i=1}^{n} p_i' - p \right), \tag{15}$$

with p that indicates the incoming momentum.
Collinear factorisation allows us to neglect quantum interferences and to separate the events of the shower, so that a splitting process is not influenced by what happens next. Therefore, we get a sequence of emissions whose probability does not depend on the past history of the system: a so called Markov chain.
If we consider i splitting processes, we can use the factorization properties of the amplitude to show that the final cross section goes as:

$$\sigma_0 \alpha_s^i \int \frac{dt_1}{t_1} ... \frac{dt_n}{t_n} \times \theta(t^H > t_1 > t_2 > ... > t_i > t^c) = \sigma_0 \frac{1}{i!} \alpha_s^i \ln^i \left(\frac{t^H}{t^c} \right), \tag{16}$$

where θ takes on the value of one if the argument is true, otherwise zero. Because of this reason, the collinear approximation is sometimes called leading log approximation.

2.3 Sudakov form factor

In the case of parton branching for partons of type $a \in \{q, g\}$, the Sudakov form factor Δ is defined as the probability of non emission of a. The Sudakov form factor corresponds to a Markov process: it only takes into account the value of the previous state. This can be done due to collinear factorisation. The Sudakov form factor will be the driving term of the probabilistic simulation of our toy parton shower.

We start from the differential probability that the splitting $a \to bc$ will occur between t and $t + dt$:

$$d\mathcal{P}_{a\to bc}(t) = \frac{dt}{t}\frac{\alpha_s(t)}{2\pi}\int_0^{2\pi}\frac{d\varphi}{2\pi}\int_{z_-}^{z_+} dz\, P_{a\to bc}(z), \tag{17}$$

where $P_{a\to bc}(z)$ is a splitting function and depends on z which represents the energy fraction of the splitting and $\alpha_s(t)$ is the running coupling constant of the QCD. The limits of the z-integration, $z_\pm$, result from the conservation of the four-momentum and depend on how the details of the kinematics are implemented.
We choose to order the shower with respect to the transverse momentum p_T, i.e. $t = p_T$. When the parton b becomes collinear to the parton c, the integration on $\frac{dp_T}{p_T}$ implies a divergence. This problem is solved setting a lower cut-off $p_T^c > 0$.
The shower proceeds towards progressively smaller values of the p_T. Therefore, we get a decreasing succession of transverse momenta, $p_T^H > p_{T,1} > .. > p_{T,i} > .. > p_T^c$.

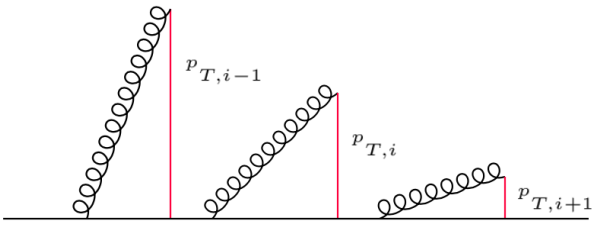

The probability of no emission between p_T and $p_T + dp_T$ is simply $1 - d\mathcal{P}_{a\to bc}(p_T)$. Assuming n splitting processes between p_T^H (that provides an upper cut-off) and a generic $p_T^c < p_T < p_T^H$ have occurred, we can define the Sudakov form factor as the probability that the parton evolves between p_T and p_T^H without any branching:

$$\begin{aligned}\Delta(p_T^H, p_T) &= \prod_{i=0}^{n-1}\left[1 - \frac{dp_{T_i}}{p_{T,i}}\frac{\alpha_s(p_{T,i})}{2\pi}\int_0^{2\pi}\frac{d\varphi}{2\pi}\int_{z_-}^{z_+} dz\, P_{a\to bc}(z)\right] \qquad p_{T,i} = \frac{i}{n}(p_T^H - p_T)\\ &= \exp\left[-\int_{p_T}^{p_T^H}\frac{dp'_{T,i}}{p'_{T,i}}\frac{\alpha_s(p'_{T,i})}{2\pi}\int_0^{2\pi}\frac{d\varphi}{2\pi}\int_{z_-}^{z_+} dz\, P_{a\to bc}(z)\right].\end{aligned} \tag{18}$$

2.4 The veto algorithm

Often the integral of the splitting kernels of the Sudakov factor are difficult to solve analytically or with Monte Carlo methods. The veto algorithm provides a very efficient solution.

Let $f(t)$ be the splitting kernel of the parton shower, integrated over the variable z, and

therefore depending only on the evolution variable t. The differential probability that a single splitting has occurred between t and the upper cut-off t^H is:

$$\mathcal{P}(t) = \frac{d}{dt}(1 - \Delta(t^H, t)) = -\frac{d}{dt} \exp\left[-\int_t^{t^H} f(t')dt' \right] = f(t) \exp\left[-\int_t^{t^H} f(t')dt' \right], \quad (19)$$

where the Sudakov $\Delta(t^H, t)$ is:

$$\Delta(t^H, t) = \exp\left[-\int_t^{t^H} f(t')dt' \right]. \quad (20)$$

If we know the inverse $F(t)^{-1}$ of the primitive function of $f(t)$, we can find the value of t in the following way:

$$\int_t^{t^H} \mathcal{P}(t')dt' = \Delta(t^H, t^H) - \Delta(t^H, t) = 1 - \exp\left[-\int_t^{t^H} f(t')dt' \right] = 1 - r \quad (21)$$

$$\Rightarrow \Delta(t^H, t) = r. \quad (22)$$

The solution is:

$$F(t) - F(t^H) = \ln(r) \quad \Longleftrightarrow \quad t = F^{-1}(\ln(r) + F(t^H)) \quad (23)$$

where r is a random number uniformly distributed between 0 and 1.

The key point of veto algorithm comes into play when considering a more complicated and elaborated splitting function. Even if we do not know the function $F(t)$, we can generate points according to a majorant function $g(t)$ of $f(t)$ with a known primitive $G(t)$.
The method consists in the following three points:

- generate points according to $g(t)$ using $t_i = G^{-1}(\ln(r) + G(t_{i-1}))$;
- compare a new r with the acceptance probability $a \equiv \frac{f(t_i)}{g(t_i)}$. Reject t_i if the ratio is smaller or equal to r;
- if $a > r$, accept t_i as the final answer.

3 Simplified model: single parton splitting

A first approach to the parton shower is obtained by considering only a quark that emits gluons and thus loses energy. This model can be visualised in a quark-antiquark annihilation followed by the generation of a Z-boson, where the moving quark decelerates and emits gluons. The sum of the transverse momenta of these emissions will correspond to the transverse momenta of the boson Z.
We consider the splitting of a quark with energy E into a gluon with energy $(1-z)E$ and another quark with energy zE. We set a maximal value of $p_T^H = 100$ GeV to the transverse momentum; and also a minimal value $p_T^c = 1$ Gev, which tells us when we have to stop to generate events.

In the case of the $q \to qg$ branching, we use the Altarelli-Parisi splitting function $P_{qq}(z) = C_F \frac{1+z^2}{1-z}$, where $C_F = 4/3$ represents the quark Casimir. As we can see, this function has a problem for z going to 1, which is the soft limit. The energy of the radiated gluon goes to zero and this leads to an infrared divergence in QCD. We are not interested in this case and we deal only with the collinear limit.

We compute the integral on z of the splitting function, using $z_- = 0$ and $z_+ = 1 - \frac{2\,p_T}{p_T^H}$ (see Appendix A.1):

$$\begin{aligned}
\int_0^{1-\frac{2\,p_T}{p_T^H}} dz\,\frac{1+z^2}{1-z} &= \int_0^{1-\frac{2\,p_T}{p_T^H}} \frac{dz}{1-z} + \int_0^{1-\frac{2\,p_T}{p_T^H}} dz\,\frac{z^2}{1-z} \\
&= -\ln\left(\frac{2\,p_T}{p_T^H}\right) - \int_1^{\frac{2\,p_T}{p_T^H}} du\,\frac{(1-u)^2}{u} \\
&= -\ln\left(\frac{2\,p_T}{p_T^H}\right) - \int_1^{\frac{2\,p_T}{p_T^H}} du\,(u-2+\frac{1}{u}) \\
&= -2\ln\left(\frac{2\,p_T}{p_T^H}\right) - \frac{2\,p_T^2}{(p_T^H)^2} + \frac{4\,p_T}{p_T^H} - \frac{3}{2}.
\end{aligned} \tag{24}$$

In the collinear limit the leading logarithmic (LL) accuracy is sufficient and therefore the Sudakov factor assumes the following formula:

$$\Delta(p_T^H, p_T) = \exp\left\{\frac{4\,C_F}{\pi}\int_{p_T}^{p_T^H}\frac{dp'_T}{p'_T}\alpha_s(p'_T)\,\ln\left(\frac{p'_T}{p_T^H}\right)\right\}. \tag{25}$$

Remember that the Sudakov form factor is a probability of independent events, therefore the probability of two events occurring is described by the product of the probability of the single event happening. For this reason, the Sudakov form factor can also be written as:

$$\Delta(p_T^H, p_T) = \prod_i \Delta(p_{T,i}, p_{T,i+1}) \tag{26}$$

with $p_T^c < p_T < p_{T,i+1} < p_{T,i} < p_{T,0} = p_T^H$ and

$$\Delta(p_{T,i}, p_{T,i+1}) = \exp\left[\frac{4C_F}{\pi}I\right] \equiv \exp\left[\frac{4C_F}{\pi}\int_{p_{T,i+1}}^{p_{T,i}}\frac{dp'_T}{p'_T}\alpha_s(p'_T)\ln\left(\frac{p'_T}{p_{T,i}}\right)\right]. \tag{27}$$

At first, we consider the case in which the strong coupling is fixed $\alpha_s = 0.4$. This is a useful step, because later we will deal also with the case of the running coupling constant and take some of these results to use the veto method.

3.1 The case of fixed α_s

We set a fixed value of 0.4 to the strong coupling constant α_s. This allows us to simplify equation (27).

$$\begin{aligned}\Delta(p_{T,i}, p_{T,i+1}) &= \exp\left[\frac{4C_F\alpha_s}{\pi}\int_{p_{T,i+1}}^{p_{T,i}}\frac{dp'_T}{p'_T}\ln\left(\frac{p'_T}{p_{T,i}}\right)\right] \\ &= \exp\left[-\frac{2C_F\alpha_s}{\pi}\ln^2\left(\frac{p_{T,i+1}}{p_{T,i}}\right)\right].\end{aligned} \tag{28}$$

Since in this case we exactly know the primitive of the integrand function of equation (28) and its inverse, we recall equations (22) and (23). Therefore, for an uniformly distributed random number $r_{i+1} \in [0,1]$, we obtain:

$$\Delta(p_{T,i}, p_{T,i+1}) = r_{i+1} \quad \Longrightarrow \quad p_{T,i+1} = p_{T,i}\exp\left[\sqrt{-\frac{\pi}{2C_F\alpha_s}\ln(r_{i+1})}\right]. \tag{29}$$

Using equation (26), one can see for an arbitrary $j \in \{1, 2, ..\}$ that:

$$\Delta(p_T^H, p_{T,j}) = \prod_{k=1}^{j}\Delta(p_{T,k-1}, p_{T,k}) = \prod_{k=1}^{j} r_k > r_{j+1}\cdot\prod_{k=1}^{j} r_k = \Delta(p_T^H, p_{T,j+1}) \tag{30}$$

where $p_{T,0} \equiv p_T^H$.
Since the expression represented in equation (29) is a function in the domain $[0,1]$ and it is monotone increasing, one produces a decreasing succession of transverse momenta p_T.

3.2 The case of running α_s

The running of the $\alpha_s(p_T)$ is obtained as a solution of the renormalisation group equation (RGE):

$$\alpha_s(p_T) = \frac{\alpha_s(M_Z)}{1 + 2\alpha_s(M_Z)\beta_0\ln(\frac{p_T}{M_Z})} = \frac{1}{2\beta_0\ln(\frac{p_T}{\Lambda})} \tag{31}$$

$\beta_0 = \frac{11C_A - 2n_F}{12\pi}$ is the first order coefficient of the QCD beta function and

$$\Lambda = M_Z\exp\left[-\frac{1}{2\alpha_s(M_Z)\beta_0}\right],$$

is the scale corresponding to the Landau pole $1 + 2\alpha_s(M_Z)\beta_0\ln(\frac{\Lambda}{M_Z}) = 0$.
If we use a running coupling constant, the inverse of the primitive of the integrand of I (equation (27)) is more difficult to find and we can no longer use equation (22) and (23) to find the succession of transverse momenta. Therefore, we have two possibilities: the bisection method and the veto algorithm.

3.2.1 Bisection method

Since also the Sudakov factor is a probability, its value is always between zero and one. Moreover, also the random number r is contained in the range $[0,1]$, this allows us to be sure that the help function

$$h(p_{T,i}, p_{T;i+1}, r_{i+1}) \equiv \Delta(p_{T,i}, p_{T;i+1}) - r_{i+1} \tag{32}$$

crosses the x-axis for certain values of $p_{T,i+1}$. With the bisection method we can identify the zeros of the function h and consequently construct the decreasing succession of transverse momenta.

The idea is to bisect repeatedly the interval where the function is defined and then select the subinterval in which the function changes sign. Setting a minimal tolerance to the length on the subinterval, we can identify the root of the function.
To use this method we need to solve the integral I of the Sudakov as follows:

$$\begin{aligned} I &= \int_{p_{T,i+1}}^{p_{T,i}} \frac{dp'_T}{p'_T}\alpha_s(p'_T)\ln\left(\frac{p'_T}{p_{T,i}}\right) = \frac{1}{2\beta_0}\int_{\frac{p_{T,i+1}}{p_{T,i}}}^{0}\frac{dx}{x}\frac{\ln(x)}{\ln(x)+\ln(\frac{p_{T,i}}{\Lambda})} \\ &= \frac{1}{2\beta_0}\int_{\ln(\frac{p_{T,i+1}}{p_{T,i}})} dy\frac{y}{y+\ln(\frac{p_{T,i}}{\Lambda})} = \frac{1}{2\beta_0}\int_{\ln(\frac{p_{T,i+1}}{p_{T,i}})} dy\left[1-\frac{\ln(\frac{p_{T,i}}{\Lambda})}{y+\ln(\frac{p_{T,i}}{\Lambda})}\right] \\ &= -\frac{1}{2\beta_0}\left[-\ln\left(\frac{p_{T,i}}{\Lambda}\right)\ln\left(\ln\left(\frac{p_{T,i+1}}{\Lambda}\right)\right)+\ln\left(\frac{p_{T,i+1}}{p_{T,i}}\right)+\ln\left(\frac{p_{T,i}}{\Lambda}\right)\ln\left(\ln\left(\frac{p_{T,i}}{\Lambda}\right)\right)\right]. \end{aligned} \tag{33}$$

3.2.2 Veto algorithm

As explained before, we need to identify a majorant of the integrand of I. In this case we have:

$$\begin{aligned} f(p_{T,i},p'_T) \equiv \frac{1}{p'_T}\alpha_s(p'_T)\ln\left(\frac{p'_T}{p_{T,i}}\right) &< \frac{1}{p'_T}\max_{p'_T\in[p_T^c,p_T^H]}\{\alpha_s(p'_T)\}\ln\left(\frac{p'_T}{p_{T,i}}\right) \\ &= \frac{1}{p'_T}\alpha_s(p_T^c)\ln\left(\frac{p'_T}{p_{T,i}}\right) \equiv g(p_{T,i},p'_T) \end{aligned} \tag{34}$$

which corresponds to the case explained in section 3.1 where α_s is constant. We start from p_T^H and we continue to generate points according to equation (23), since we know the primitive of $g(p_{T,i},p'_T)$, which is

$$G(p_{T,i},p_{T,i+1}) = -\frac{1}{2}\ln^2\left(\frac{p_{T,i+1}}{p_{T,i}}\right). \tag{35}$$

When p_T^c is reached, we stop generating points and we select them by using the additional acceptance rate

$$a \equiv \frac{f(p_{T,i},p_{T,i+1})}{g(p_{T,i},p_{T,i+1})} = \frac{\alpha_s(p_{T,i+1})}{\alpha_s(p_T^c)}. \tag{36}$$

Then we take an uniformly random number r, and if $a > r$ we accept $p_{T,i+1}$, otherwise we reject it.

3.3 Observables

In both cases, at the end of the simulation, lists containing decreasing succession of transverse momenta are generated. The first observable that we measure is the total recoil generated by each splitting process, i.e the sum of the modules of the transverse momenta of each branching process:

$$P_T^{(k)} \equiv \sum_i p_{T,i}^{(k)} \tag{37}$$

where k simply labels a single simulation.
Figure (2) shows the distributions of the sum of the transverse momenta. The left histogram, obtained with $\alpha_s = 0.4$ as described in section 3.1, has a peak around 120 GeV (which is above the upper cut-off) and a spread of ~ 80 GeV. The right histogram is less symmetric and shifted to the left; its peak is positioned around 30 GeV, and the distribution has a spread of ~ 40 GeV.

The reason behind these differences is the behaviour of the strong coupling constant at different p_T: $\alpha_s(p_T)$ decreases at large values of the transverse momentum, while it is large at low values of p_T. In the case of fixed α_s, each event is weighted in the same way, hence a flatter, shifted distribution is observed. When the coupling constant runs, all the radiations are weighted differently: the probability with which they occur is smaller at larger p_T.

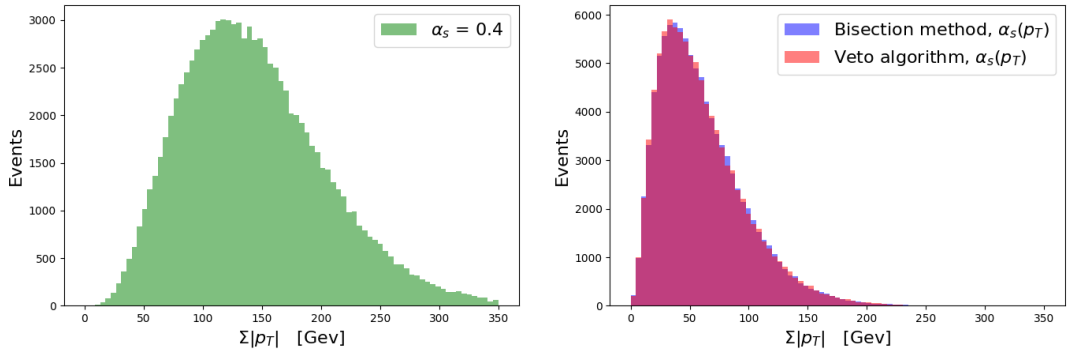

Figure 2: Distribution of the sum of the modules of the generated transverse momenta. Left panel $\alpha_s = 0.4$ and right panel for running coupling constant. Computed with $N = 10^5$ events simulated.

Taking into account also the direction of each recoil of the splitting, as a first approximation one can find the vector of the transverse momentum using an angle φ_i uniformed distributed in $[0, 2\pi]$:

$$\vec{p}_{T,i} = p_{T,i}\cos(\varphi_i)\hat{e}_x + p_{T,i}\sin(\varphi)\hat{e}_y, \tag{38}$$

so that the vector of the total transverse momentum for the k-th simulation is obtained

$$\vec{P}_T^{(k)} \equiv P_{T,x}^{(k)}\hat{e}_x + P_{T,y}^{(k)}\hat{e}_y = \sum_i p_{T,i}^{(k)}\cos(\varphi_i^{(k)})\hat{e}_x + p_{T,i}^{(k)}\sin(\varphi_i^{(k)})\hat{e}_y. \tag{39}$$

This transverse momentum must be balanced by the one of the Z-boson, i.e.:

$$\vec{P}_T^{(k)} = -\vec{P}_T^{(Z)}. \tag{40}$$

Figure (3) displays the distributions of the modules of the vector sum of the transverse momenta

$$|\vec{P}_T^{(k)}| = \sqrt{\left(P_{T,x}^{(k)}\right)^2 + \left(P_{T,y}^{(k)}\right)^2}. \tag{41}$$

The histograms have peaks at smaller value than in the previous figure, they are shifted to the left and the histogram computed with fixed α_s is more asymmetric than the previous one. This is because with the vector summing there are cancellations or attenuations of certain transverse momenta. However, as before, the shape of the distributions is influenced by the running coupling constant. In the left panel, with $\alpha_s = 0.4$, there is a peak at 30 GeV and the spread of the distribution is ~ 40 GeV; the right panel shows a distribution with a peak at 10 GeV and a spread of ~ 30 GeV.

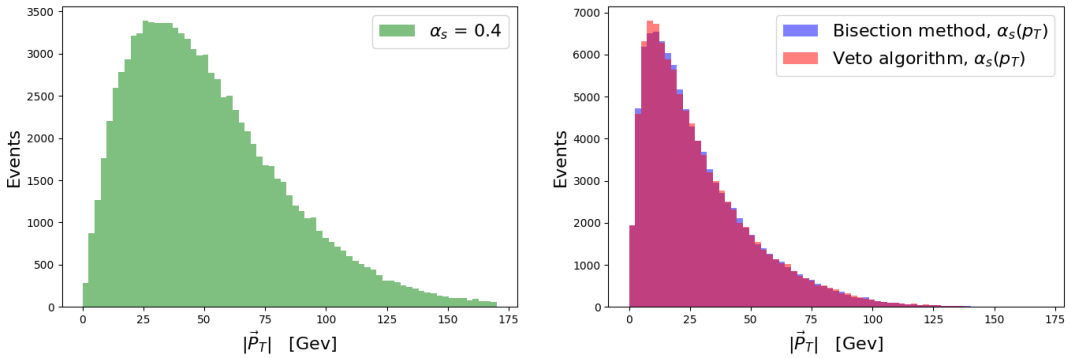

Figure 3: Distribution of the modules of the vector sum of the transverse momenta. Both histograms are computed by simulating $N = 10^5$ events. The left one with $\alpha_s = 0.4$, while α_s runs in the right one.

By comparing the bisection method and the veto algorithm, described in section 3.2, we expect the same results. In fact, despite the bisection method being slower to compute the observables, the distributions on the right of figures (2) and (3) match perfectly. The veto algorithm is as accurate as the bisection method, although it excludes some events, which makes it faster.

4 Dipole showers

Whereas in the previous section we considered only a single splitting, in this one we will analyse all possible splittings that the various branches can do. We are interested in the whole kinematics of the parton shower, which is described by the four momenta of each particle. The process has to conserve the four-momentum, and since we are dealing with massless particles, to meet this requirement we decide to employ dipole shower. The idea is to identify in each splitting a possible particle, called spectator s, which can absorb the recoil of the emitted daughters. The introduction of the spectator s allows us also to conserve the color and other quantum numbers.
At each vertex one can see the emitter which decays into two daughters b and c; by linking a spectator s to the daughters, the dipole b,c and s is formed. Each dipole must be associated with a kinematics and with a splitting probability.
Given the previous momentum of the emitter $\tilde{p}_a$, the one of the spectator $\tilde{p}_s$, two radiation variables z,y and an azimuthal angle φ, one is able to produce a list containing the momenta of the daughter p_b, p_c and the new one of spectator p_s.

The initial momenta of the quark and antiquark generated by the hard process can be extrapolated from section 2.1. According to the conservation law of color, flavor and four-momentum the initial particles will split in less energetic gluons, quarks or antiquarks. Where and when a particle should be added to a certain branch is also determined by the randomness of the algorithm, then the energy is decreased and the process continues until the energy reaches a minimum limit.

4.1 The Kinematics

With the introduction of the spectator s, at each vertex the following decay is observed:

$$a(\tilde{p}_a) + s(\tilde{p}_s) \to b(p_b) + c(p_c) + s(p_s). \tag{42}$$

Note that the spectator only changes its momentum, absorbing the recoil of the other particles. The energy splitting parameter z describes the quantity of energy of the emitter parton which is distributed between the daughters, while the recoil parameter y represents the part of energy that the spectator gives to the daughters in order to absorb the recoil. They are called "radiation variables" and are defined as follows:

$$\begin{aligned} z &= \frac{p_b p_s}{p_b p_s + p_c p_s} \\ y &= \frac{p_b p_c}{p_b p_c + p_b p_s + p_c p_s}. \end{aligned} \tag{43}$$

Now we can map the kinematic variables into physical momenta:

$$p_b = z\tilde{p}_a + (1-z)y\tilde{p}_s + k_T \tag{44}$$
$$p_c = (1-z)\tilde{p}_a + zy\tilde{p}_s - k_T \tag{45}$$
$$p_s = (1-y)\tilde{p}_s, \tag{46}$$

where k_T represents the momentum transverse to both $\tilde{p}_a$ and $\tilde{p}_s$ and fulfils the following relations:

$$\begin{aligned} k_T^2 &= -2\tilde{p}_a\tilde{p}_s zy(1-z) \\ k_T^2 &= -\vec{k}_T^2 < 0 \\ \tilde{p}_a k_T &= 0 = \tilde{p}_s k_T. \end{aligned} \tag{47}$$

The first equation follows from the fact that all the involved partons are massless, and therefore for each parton of the shower $p^2 = 0$.

To find k_T, a boost transformation Λ to the center-of-mass frame $\tilde{p}_a + \tilde{p}_s$ is used. Given an arbitrary momentum q, this transformation boosts it in the frame where $\tilde{p}_a + \tilde{p}_s$ is at rest.

$$\Lambda: \quad q \equiv \begin{pmatrix} q^0 \\ \vec{q} \end{pmatrix} \longrightarrow \begin{pmatrix} v_1 \\ \vec{q} - \lambda_1(\vec{\tilde{p}}_a + \vec{\tilde{p}}_s) \end{pmatrix} \equiv q^{CM}, \tag{48}$$

where

$$v_1 \equiv \frac{q \cdot (\tilde{p}_a + \tilde{p}_s)}{\sqrt{s}} \qquad \lambda_1 \equiv \frac{q^0 + v_1}{\sqrt{s} + \tilde{p}_a^0 + \tilde{p}_s^0}$$

and $s = (\tilde{p}_a + \tilde{p}_s)^2$ is the center-of-mass energy.

In this frame the momenta of the spectator and of the emitter are boosted as follows:

$$\tilde{p}_a^{CM} = \Lambda \tilde{p}_a = \frac{\sqrt{s}}{2} \begin{pmatrix} 1 \\ \hat{p} \end{pmatrix} \qquad \text{and} \qquad \tilde{p}_s^{CM} = \Lambda \tilde{p}_s = \frac{\sqrt{s}}{2} \begin{pmatrix} 1 \\ -\hat{p} \end{pmatrix}, \tag{49}$$

$\vec{p}$ is the unit vector pointing in the same direction of $\vec{\tilde{p}}_a$ and it is spanned by two unit vectors $\hat{e}_1$ and $\hat{e}_2$. We assign an azimuthal angle φ to the the transverse momentum which can be written in the center-of-mass frame in terms of the unit vectors as follows:

$$k_T^{CM} = \cos(\varphi)\hat{e}_1 + \sin(\varphi)\hat{e}_2. \tag{50}$$

Now that we can return in the initial frame, we define the inverse of Λ:

$$\Lambda^{-1}: \quad q^{CM} \equiv \begin{pmatrix} q^{0,CM} \\ \vec{q}^{CM} \end{pmatrix} \longrightarrow \begin{pmatrix} v_2 \\ \vec{q}^{CM} + \lambda_2(\vec{\tilde{p}}_a^{CM} + \vec{\tilde{p}}_s^{CM}) \end{pmatrix} \equiv q \tag{51}$$

with

$$v_2 \equiv \frac{q^{0,CM}(\tilde{p}_a^{0,CM} + \tilde{p}_s^{0,CM}) + \vec{q}^{CM} \cdot (\vec{\tilde{p}}_a^{CM} + \vec{\tilde{p}}_s^{CM})}{\sqrt{s}}$$

and

$$\lambda_2 \equiv \frac{q^{0,CM} + v_2}{\sqrt{s} + \tilde{p}_a^{0,CM} + \tilde{p}_s^{0,CM}}$$

Finally we get:

$$k_T = \Lambda^{-1} k_T^{CM}. \tag{52}$$

4.2 The splitting functions

The branching processes that take place at the vertices are described by the splitting functions. In the case of our simulation, we need three splitting functions related to (final state) dipoles:

$$\begin{aligned} P_{qq} &\equiv \mathcal{K}_{qg,s}^{FF} = C_F \left[\frac{2}{1 - z(1-y)} - (1+z) \right] \\ P_{gg} &\equiv \mathcal{K}_{gg,s}^{FF} = \frac{C_A}{2} \left[\frac{2}{1 - z(1-y) - 2 + z(1-z)} \right] \\ P_{gq} &\equiv \mathcal{K}_{q\bar{q},s}^{FF} = \frac{T_R}{2}[1 - 2z(1-z)] \end{aligned} \tag{53}$$

here we have taken into account the normalisation due to the number of spectator $1/N_{spec}$. In order to apply the veto algorithm, in a similar way as done before, we need to find majorant

functions and their primitive. Since $0 < y < 1$ we get the following functions and integrals:

$$
\begin{aligned}
P_{qq}(z,y) < \mathcal{G}_{qq}(z) &\equiv C_F \frac{2}{1-z}, & G_{qq}(z_-,z_+) &\equiv \int_{z_-}^{z_+} \mathcal{G}_{qg}(z)\,dz = 2\,C_F\,\log\left(\frac{1-z_-}{1-z_+}\right),\\
P_{gg}(z,y) < \mathcal{G}_{gg}(z) &\equiv C_A \frac{1}{1-z}, & G_{gg}(z_-,z_+) &\equiv \int_{z_-}^{z_+} \mathcal{G}_{gg}(z)\,dz = C_A\,\log\left(\frac{1-z_-}{1-z_+}\right),\\
P_{gq}(z,y) < \mathcal{G}_{gq}(z) &\equiv \frac{T_R}{2}, & G_{gq}(z_-,z_+) &\equiv \int_{z_-}^{z_+} \mathcal{G}_{gq}(z)\,dz = \frac{T_R}{2}(z_+ - z_-).
\end{aligned}
\tag{54}
$$

4.3 Parton shower event generator

The shower is ordered in the transverse momentum, i.e. $t \equiv |k_T|^2$. Starting from the ordering variable $t > t^c = 1$ GeV, the algorithm searches among all the final state particles for a possible spectator s and connect its color with the one of the emitter a. Indeed, one has to be careful also about the color flow because in each vertex the color has to be conserved, and therefore not all branching process are allowed if the colour conservation is not met. Moreover, for the branching $g \to gg$ we need to decide on the new color flow of the finale state; this is done with the leading color (LC) approximation.

As a next step, the appropriate splitting function P_{bc} must be selected and the boundaries $z_\pm$ have to be found in order to use the primitive G_{bc} of the majorant function $\mathcal{G}_{bc}$.
To reach the maximal and minimal value of z, one sets t to its minimum value and $y = 1$ and inverts equation (47):

$$
z_\pm = \frac{1}{2} \pm \frac{1}{2}\sqrt{1 - \frac{2t^c}{\tilde{p}_a \tilde{p}_s}}. \tag{55}
$$

Finally, we generate values of the ordering variable t according to the majorant function $\mathcal{G}_{bc}$. If its result is the highest means that we have found the most probable emission. We therefore memorize all the parameters of the new emission; that means all the information about the emitter and the spectator, the values of the z-boundaries and the kind of splitting function. In practice, the algorithm puts all possible splitter-spectators pairs and splitting functions into competition by generating values of t, and the winner will construct the splitting kinematics. For each splitting functions we have also to find a function that, given a random number r, describes the distribution of the z between z_- and z_+. These functions were found by solving:

$$
\frac{G_{bc}(z_-,z) - G_{bc}(z_-,z_-)}{G_{bc}(z_-,z_+) - G_{bc}(z_-,z_-)} = r
$$

with solution

$$
\begin{aligned}
z_{qq} &= 1 + (z_+ - 1)\left(\frac{1-z_-}{1-z_+}\right)^r\\
z_{gg} &= 1 + (z_+ - 1)\left(\frac{1-z_-}{1-z_+}\right)^r\\
z_{gq} &= (z_+ - z_-)\,r + z_-.
\end{aligned}
\tag{56}
$$

The value of z is generated with the help of these functions, this means that the choice of how much energy should be distributed to a daughter parton is completely random, whereas an expression for y which depends on t can be found by inverting $t = 2\tilde{p}_a\tilde{p}_s yz(1-z)$:

$$
y = \frac{t}{2\tilde{p}_a\tilde{p}_s z(1-z)}. \tag{57}
$$

It remains only to apply the veto method in order to select a valid phase space point (t, z, φ). We know the majorant functions and their primitive of all the splitting kernels, therefore we only have to compute the acceptance probability a:

$$a = \frac{(1-y)\alpha_s(t)P_{bc}(z,y)}{\alpha_s(t_0)\mathcal{G}_{bc}(z)} \tag{58}$$

where the term $(1-y)$ is a phase-space factor.
We accept t only if a is larger than a random number r. In the end, we find a list of parameters containing information about the momentum of a and s and the value of the radiation variables z, y. We take a random azimuthal angle $\varphi \in [0, 2\pi]$, and using equations (44)-(46) we get the new momenta of the spectator and of the emitter. Starting from here we are ready to simulate another emission until we reach the minimal value of the evolution variable.

At the end of the algorithm one has the list containing information on the flavour, momenta and color of each particle.

4.4 Observables

4.4.1 k_T jet-clustering algorithm

Quarks and gluons cannot propagate freely because of colour confinement, and are therefore observed as jets of colorless particles or hadrons. Jets are flows of energy in a restricted angular region and they are the signals that are measured in the detectors. Depending on how the jet is defined and constructed, different results are obtained. This is mainly done by jet algorithms.
Consider a parton i with energy E_i and with distance d_{iB} from the beam. In each jet algorithm one has to set the distance d_{iB} and define a metric d_{ij} between the partons i and another parton j with energy E_j. In particular we use a clustering algorithm in the spherical coordinates with the following metric:

$$d_{ij} = \min(E_i^{2p}, E_j^{2p})\frac{(1-\cos\theta_{ij})}{(1-\cos R)} \qquad\qquad d_{iB} = E_i^{2p}, \tag{59}$$

The parameter p controls the impact of the power of the energy of the parton, in this case $p = -1$ which means that the less energetic partons are left aside. On the other hand if $p = 1$ soft partons are preferred.
The radius of the cone jet, which has a circular profile in the 3 dimensional sphere, is regulated by the parameter R. In this algorithm the value of R is between 0.1 and 0.2.
The algorithm consists of finding the minimum of d_{ij}; if it is smaller than $d_{i,B}$ the two particles are clustered in a new pseudo-particle and continue with another particle. Otherwise, particle i is a final state jet, called "inclusive jet", and one continue, by removing it to the list of the particles.

If we increase the value of R up to 1 or more, we talk about "fat" jets. As one can observe in figure (4), the number of jets decreases as the value of the parameter R increases. This is due to the fact that "fat" jets include more final state partons; because by increasing the parameter R, two particles with a larger angle θ_{ij} between them can be clustered.

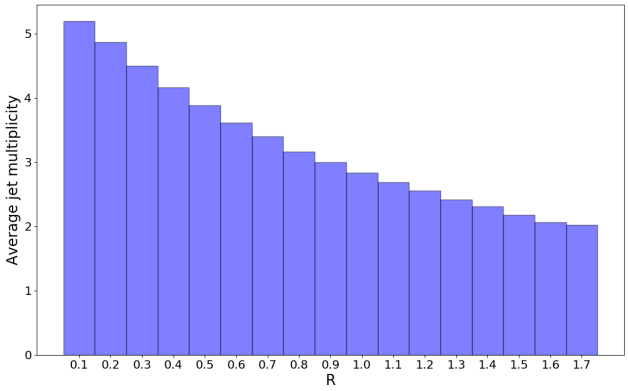

Figure 4: Average jet multiplicity generated with different values of the parameter R after $N = 10^4$ events.

Other parameters can affect the he average jet multiplicity. Indeed, by increasing the center of mass energy, a larger number of more energetic partons are produced, allowing the diffusion and the branching in different directions. In figure (5), a logarithmic growth of the average jet multiplicity as a function of $\sqrt{s}$ is observed.

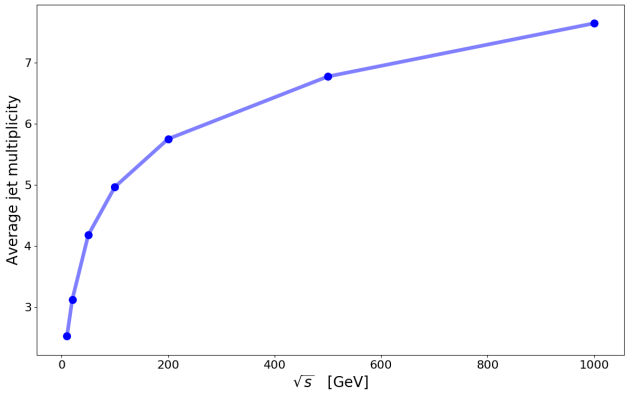

Figure 5: The center of mass energy influences the average jet multiplicity. Plot computed with $R = 0.2$ and $N = 10^4$ events.

In the following, we perform two measurements regarding the Z-boson, which is the mediator of the $q\bar{q}$ pair production. The value of the parameter R is fixed to 0.2 and the center of mass energy is set at $\sqrt{s} = M_Z$.
Using these parameters the average jet multiplicity at the end of the clustering is between 4 and 5 (figure (6)).

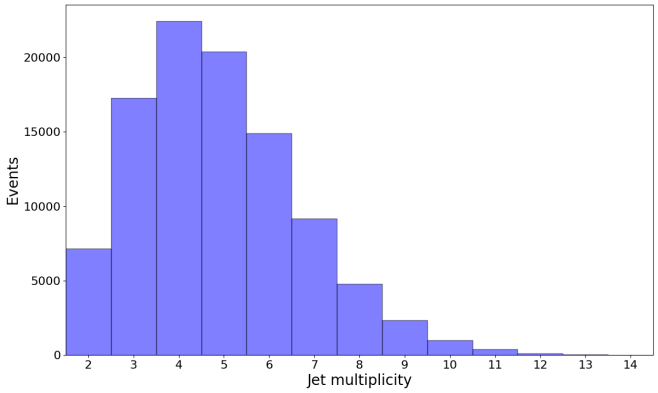

Figure 6: Jet multiplicity at $\sqrt{s} = M_Z$, computed after $N = 10^5$ simulations and with a parameter of $R = 0.2$

Consider the two jets with larger transverse momentum with four-momentum p_1 and p_2. Using the following equation, the mass of the Z-boson can be found:

$$M_Z = (p_1^0 + p_2^0)^2 - \sum_{i \in \{x,y,z\}} (p_1^i + p_2^i)^2. \tag{60}$$

The distribution of the Z-boson mass shown in figure (7) is generated by excluding all the events with only 2 final jets, which represents 7% of the simulations. This is because the distribution of these events is trivial, i.e. they give exactly the mass of the Z-boson. We are interested in the distribution of the mass given by the simulations with 3 or more jets. The histogram has a linear trend towards the peak, which is at $\sim$ 89 GeV, and then descends around the Z-boson mass of 91.2 GeV.

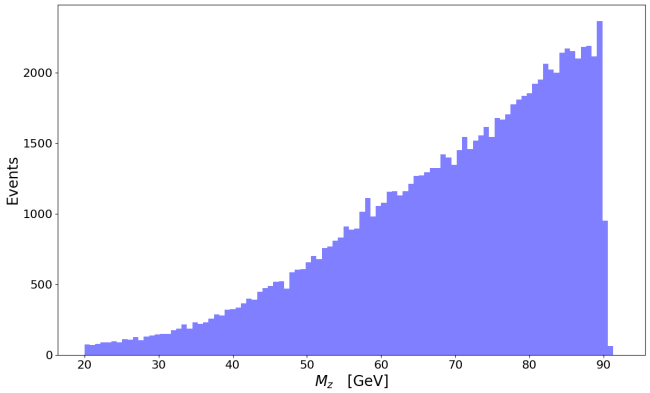

Figure 7: Distribution of M_Z, developed with $\sqrt{s} = M_Z$, $R = 0.2$, and by generating $N = 10^5$ events. All events with only 2 final jets have been removed.

The distribution of the module of the transverse momentum is displayed in figure (8) and it is obtained using the first two hard jets as before:

$$|p_T^Z| = \sqrt{(p_1^x + p_2^x)^2 + (p_1^y + p_2^y)^2} \tag{61}$$

also in this case, 2 jets events are removed.

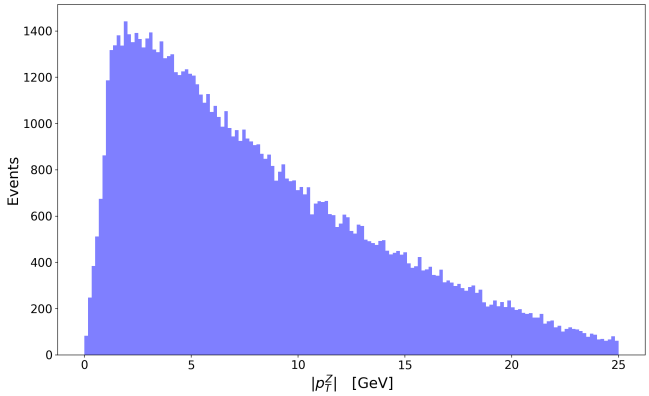

Figure 8: Distribution of the module of the transverse momentum of the Z-boson developed with $R = 0.2$, $N = 10^5$ and $\sqrt{s} = M_Z$

4.4.2 Thrust distribution

One interesting event-shape variable that can be measured is the thrust, which is defined with the following formula:

$$T = \max_{\vec{n}} \frac{\sum_i |\vec{n} \cdot \vec{p}_i|}{\sum_i |\vec{p}_i|}, \tag{62}$$

where $|\vec{n}| = 1$ and $\vec{p}_i$ is the momentum of a final state parton. The different values that T can take, give us information about how the various branches of the shower are distributed in the space with respect to an axis $\vec{n}$. For example, $T = 1$ means that the event is back-to-back, whereas $T = 1/2$ is when the event is spherically symmetric.
In figure 9 the distribution of T is shown. After the peak, which is located slightly below $T = 1$, a small reduction is observed. Note that we remove all the events that do not radiate, corresponding to 5% of the total simulations, which are back-to-back, i.e. their thrust value is 1. These events are present because of the lower cut-off. In particular, the Sudakov form factor between the upper and lower cut-off is larger than zero. Usually, these events are redistributed and not observed, since physically the emissions are not blocked by a cut-off.

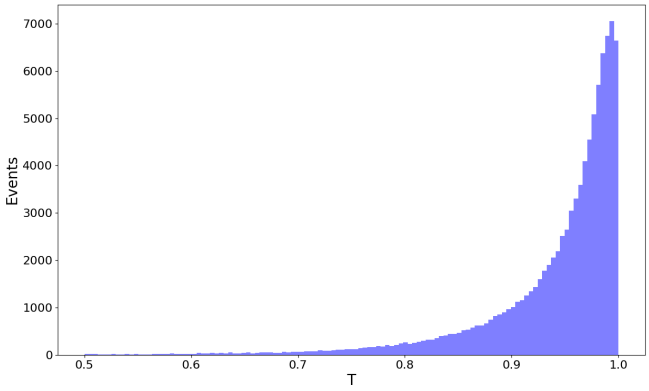

Figure 9: Thrust distribution computed with $N = 10^5$ events. Back-to-back emissions have been removed.

5 Conclusion

We started with a simplified model, in order to understand the key mechanisms of these simulations and the crucial role of the strong coupling constant α_s. Then, from a cross section at LO, a toy parton shower with LL accuracy was added. The parton shower was ordered in the transverse momentum, although at this accuracy other variables (such as angle or invariant mass) could also be used.
Later, using a jet algorithm, the mass and the transverse momentum of the boson Z was reconstructed.
In the end, the thrust distribution of the final state partons is examined: the majority of emissions were nearly back-to-back.
Furthermore, relying on models based on general characteristics of QCD, this work could be extended to the hadronization, where final state hadrons are observed.

6 References

- John Campbell, Joey Huston and Frank Krauss. *The Black Book of Quantum Chromodynamics*. Oxford University Press, 2017.
- Michael E. Peskin, Daniel V. Schroeder. *An Introduction To Quantum Field Theory*. Addison-Wesley, 1995.
- P. Nason. *Shower Monte Carlo programs*, Frascati Phys.Ser. 49 (2009) 34-67.
- A. Papaefstathiou. *How-to: Write a parton-level Monte Carlo particle physics event generator*, Eur.Phys.J.Plus 135 (2020), arXiv:1412.4677.
- T. Sjostrand, S. Mrenna and P. Z. Skands. *PYTHIA 6.4 Physics and Manual*, JHEP 05 (2006) 4:60-68, arXiv:hep-ph/0603175.
- Stefan Höche. *Introduction to parton-shower event generators*, TASI (2014) 235-295, arXiv:1411.4085v2.
- Matteo Cacciari, Gavin P. Salam and Gregory Soyez. *FastJet 3.0.0 user manual*, Eur.Phys.J.C 72 (2012) 4.5:21, arXiv:1111.6097v1.
- Vincenzo Chiochia, Günther Disserrtori, Thomas Gehrmann. *Lecture notes in Particle Physics Phenomenology 1*.

A Appendices

A.1 The limits of z-integration

Consider the kinematics associated to the production of a massive colourless object of mass M. At lowest order in perturbation theory, after the annihilation of two partons with momenta p_1 and p_2 one can observe the creation of the final state particle with momentum p_3 and mass $M = \sqrt{p_3^2}$. We consider the radiative emission with momentum k of one extra parton off one of the incoming parton. Momentum conservation yields the following equation:

$$p_1 + p_2 \to p_3 + k.$$

In the center of mass frame, the set of momenta can be written as:

$$p_{1,2} = \frac{\sqrt{s}}{2}(1, 0, 0, \pm 1), \qquad p_3 = \left(\sqrt{\vec{k}^2 + M^2}, -\vec{k}\right), \qquad k = (|\vec{k}|, \vec{k}),$$

where $s = (p_1 + p_2)^2$ and $|\vec{k}| = \sqrt{\vec{k}_T^2 + k_z^2} = \sqrt{s}/2(1 - M^2/s)$.
We identify the energy fraction $z = M^2/s$, and for a fixed value of $\vec{k}_T^2$, the maximum value that the energy fraction can reach is $z_+ = M^2/s_{min}$. Using the definition of s we see that:

$$s = (p_3 + k)^2 = M^2 + 2p_3 \cdot k = M^2 + 2\sqrt{\vec{k}^2 + M^2}|\vec{k}| + 2\vec{k}^2$$

and that the minimum is when $k_z = 0$:

$$s_{min} = M^2 + 2\sqrt{\vec{k}_T^2 + M^2}|\vec{k}_T| + 2\vec{k}_T^2.$$

Finally we get:

$$z_+ = \frac{M^2}{s} = \frac{1}{1 + \frac{2k_T}{M}\left(\sqrt{\frac{k_T^2}{M^2} + 1} + \frac{k_T}{M}\right)} \approx 1 - \frac{2k_T}{M}, \qquad k_T \equiv |\vec{k}_T|.$$

For the lower boundary we have $z_- = M^2/s_{max}$; and considering that s_{max} is the maximal energy available in the hadronic center of mass frame, we can assume that $s_{max} \gg M^2$. It follows that $z_- \approx 0$.

A.2 Differential cross section for $2 \to 2$ scattering

Consider a scattering between two particle $\mathcal{A}$, $\mathcal{B}$ with energy $E_\mathcal{A}$, $E_\mathcal{B}$ and momentum $p_\mathcal{A}$, $p_\mathcal{B}$, followed by the formation of two particle 1, 2 with energy E_1, E_2 and momentum p_1, p_2. The cross section of this process is:

$$d\sigma = \frac{1}{2E_\mathcal{A}2E_\mathcal{B}|v_\mathcal{A} - v_\mathcal{B}|}\left(\prod_{i=1}^{2}\frac{d^3p_i}{(2\pi)^3}\frac{1}{2E_i}\right)|\mathcal{M}(p_\mathcal{A}, p_\mathcal{B} \to \{p_i\})|^2(2\pi)^4\delta^{(4)}\left(p_\mathcal{A} + p_\mathcal{B} - \sum_{i=1}^{2}p_i\right)$$

where $|v_\mathcal{A} - v_\mathcal{B}|$ is the relative velocity of the beams in the laboratory frame.
To solve the integral over final-state momenta in the previous equation, we change the reference frame and we use the center of mass frame where $\vec{p}_1 = -\vec{p}_2$:

$$\int d\Phi_2 = \int \frac{dp_1\, p_1^2\, d\Omega}{(2\pi)^3 2E_1 2E_2}(2\pi)\delta(E_{cm} - E_1 - E_2)$$

with $E_1 = \sqrt{p_1^2 + m_1^2}$, $E_2 = \sqrt{p_1^2 + m_2^2}$, $p_i = |\vec{p}_i|$ and $E_{cm} = E_\mathcal{A} + E_\mathcal{B}$. The delta function gives us the possibility of further simplifying the integral:

$$\begin{aligned}\int d\Phi_2 &= \int d\Omega \frac{p_1^2}{16\pi^2 E_1 E_2}\left(\frac{p_1}{E_1} + \frac{p_1}{E_2}\right)^{-1} \\ &= \int d\Omega \frac{1}{16\pi^2}\frac{p_1}{E_{cm}}.\end{aligned}$$

The integral over $d\Omega = d\cos\theta d\varphi$ can be written simply as an integral over the polar angle:

$$\int d\Phi_2 = \int d\cos\theta \frac{1}{16\pi}\frac{2p_1}{E_{cm}}.$$

With this simplification the initial equation becomes:

$$\left(\frac{d\sigma}{d\Omega}\right)_{CM} = \frac{1}{2E_{\mathcal{A}}2E_{\mathcal{B}}|v_{\mathcal{A}} - v_{\mathcal{B}}|}\frac{p_1}{(2\pi)^2 4E_{cm}}|\mathcal{M}(p_{\mathcal{A}}, p_{\mathcal{B}} \to p_1, p_2)|^2.$$

A.3 Coefficients of the hard scattering cross section

The coefficients composing the parameters A_0 and A_1 used in section 2.1 are listed below.

fermions	Q_f	V_f	A_f
u, c, t	$+\frac{2}{3}$	$(+\frac{1}{2} - \frac{4}{3}\sin^2\theta_W)$	$+\frac{1}{2}$
d, s, b	$-\frac{1}{3}$	$(-\frac{1}{2} - \frac{2}{3}\sin^2\theta_W)$	$-\frac{1}{2}$
e, μ, τ	-1	$(-\frac{1}{2} + 2\sin^2\theta_W)$	$-\frac{1}{2}$

with $\sin^2\theta_W = 0.222246$ and θ_W indicating the Weinberg angle.
Next we define:

$$\kappa = \frac{\sqrt{2}G_f M_Z^2}{4\pi\alpha_{\text{em}}}$$
$$\chi_1(s) = \frac{\kappa s(s - M_Z^2)}{((s - M_Z^2)^2 + \Gamma_Z^2 M_Z^2)}$$
$$\chi_2(s) = \frac{\kappa^2 s^2}{((s - M_Z^2)^2 + \Gamma_Z^2 M_Z^2)}$$

where the Z boson mass and width are respectively 91.188 GeV and 2.4414 GeV; and the Fermi constant is $G_f = 1.16639 \times 10^{-5}$ GeV^{-2}.
Finally we get:

$$A_0 = Q_f^2 - 2Q_f V_\mu V_f \chi_1 + (A_\mu^2 + V_\mu^2)(A_f^2 + V_f^2)\chi_2$$
$$A_1 = -4Q_f A_\mu A_f \chi_1 + 8A_\mu V_\mu A_f V_f \chi_2.$$